

Noise resilience in path-polarization hyperentangled probe states

Akshay Kannan Sairam^{1,*} and C. M. Chandrashekar^{1,2,3,†}

¹*Quantum Optics & Quantum Information, Department of Instrumentation and Applied Physics, Indian Institute of Science, Bengaluru, India*

²*The Institute of Mathematical Sciences, C. I. T. Campus, Taramani, Chennai 600113, India*

³*Homi Bhabha National Institute, Training School Complex, Anushakti Nagar, Mumbai 400094, India*

Entanglement in more than one degree of freedom is termed as hyperentanglement and are known to have certain advantages over conventional entangled states. Most quantum systems that are used for generating entanglement and used for practical applications are not isolated from environment and are hence susceptible to noise. Quantum illumination, imaging and communication schemes that involve sending one photon from a pair of entangled photons and retaining the other pair usually involves exposing one of the photons to environmental noise. The disruptive nature of noise, degrades entanglement and other correlations which are crucial for many of these applications. In this paper we study the advantages when utilising photon pairs in certain path-polarization hyperentangled states in a noisy interaction where photons in only one of the paths are affected by noise. We model such noise and study the effect of noise on the correlations present in the hyperentangled photons. Three different methods, entanglement negativity, entanglement witnesses and Bell nonlocality are used to show the resilience of path-polarization hyperentangled probe state against noise.

I. INTRODUCTION

Quantum entanglement is a useful resource in many domains of science which harness the exotic effects of quantum mechanical systems for better performance or security in information processing, metrology and communication tasks [1, 2]. Some examples of the pioneering applications of entanglement that beat the best known classical protocols are quantum dense coding, quantum teleportation, quantum key distribution, and quantum Illumination [3–6]. Entanglement is also deemed as one of the key resources behind computational speedup in quantum computing [7]. It is an essential ingredient in device independent quantum cryptography [8]. Recently, entanglement in higher dimensions has been shown to give a better performance enhancements than conventional entanglement, like enhanced channel capacity, enhanced signal to noise ratio in quantum illumination [9, 10]. Higher dimensional entanglement has also shown the robustness of entanglement against noise in quantum communication [11–13].

Entangled photons are widely used in many applications since they can be readily generated through nonlinear processes like Spontaneous Parametric Down Conversion (SPDC) using birefringent crystal, and transmitted relatively easily [14]. Interactions with the environment can subject the quantum system to noise, which leads to a loss of entanglement, decoherence and other such disruptive effects. The transmission of one of the entangled photon pair and retention of the other, causes environmental noise to act on one of transmitted photons in the noisy path. Such a scheme is commonly adopted for example in quantum cryptographic protocols, quan-

tum illumination, quantum teleportation [3, 5]. Therefore finding ways to engineer entangled states that are robust against noise is an area of continuous research interest.

Hyperentanglement— Simultaneous entanglement between two system in more than one degree of freedom, is termed as hyperentanglement [15]. Photons can be simultaneously entangled in the multiple degrees of freedom like path, polarization, time energy and orbital angular momentum [16–20]. The presence of entanglement in more than one degree, expands the dimension of the Hilbert space that the state of the photon pair. In this work we will consider one such configuration of hyperentangled state, entanglement in path and polarization degree of freedom and show the advantages of it in the desired noisy environment where noise acts on one of the path. We use a controlled Kraus operators of bit flip, phase flip and depolarizing noise, to model the noise. Different indicators of correlations, which are entanglement negativity, entanglement witnesses, and Bell nonlocality after the action of noise are use to quantify and compare the results with conventional entangled photons. It can be seen that the path-polarization hyperentangled state retains correlations as much or better than conventional entangled photons when effected by noise.

The paper is organised as follows. In Sec. II a noise model is introduced that can be used to study scenarios like quantum cryptography, quantum illumination. In Sec. III we introduce the quantifiers of correlations we use to study the effect of noise. In Sec. IV we present the numerical results showing the robustness of path-polarization hyperentangled state against noise when compared to entanglement in one degree of freedom and conclude with remarks in Sec. V.

*Electronic address: akshaykannan@iisc.ac.in

†Electronic address: chandracm@iisc.ac.in

II. PATH-POLARIZATION ENTANGLEMENT AND NOISE MODEL

Photons in composition of polarization and path degree of freedom will have an Hilbert space composition, $\mathcal{H}_{pol} \otimes \mathcal{H}_p$ where \mathcal{H}_{pol} is spanned by the basis state $\{|H\rangle, |V\rangle\}$ representing the polarization degree of freedom and \mathcal{H}_p is spanned by the basis states $\{|0\rangle, |1\rangle\}$ representing the two paths for photons. Path-polarization hyperentangled state can be generated by first generating photons entangled in polarization degree of freedom using SPDC process and by further engineering photons paths to entangle in path degree of freedom. Appropriate post selection of the states can also be used to generate path-polarization hyperentangled states [20]. To study the effect of noise on such state, we will focus on the model noise such that it acts only on the photons present in the path $|0\rangle \in \mathcal{H}_p$. We propose a controlled noise model that affects photons in path $|0\rangle$ only, and leaves the photon in the other path unaffected.

In order to model noise in such a way, it is required that a few conditions are met. For a photon state that is coupled with the spatial mode $|0\rangle_1 |0\rangle_2$, the noise should act on both the photons. Similarly, for photon states having spatial modes, $|0\rangle_1 |1\rangle_2, |1\rangle_1 |0\rangle_2$, only single photon noise should act on the photon in $|0\rangle$, and the corresponding polarization entangled photon should remain unaffected by the noise. Finally, for photons passing through $|1\rangle_1 |1\rangle_2$, both the photons should remain unaffected.

We model noise using Kraus operator representation of noise channels. These are a set of operators that are derived from jointly evolving a state along with an environment and tracing out the environment [21]. Given a set of Kraus operators describing a single photon noise model, like bit flip, depolarizing and phase damping noise.

$$K_i^1 \equiv \{K_1, K_2, \dots, K_n\}. \quad (1)$$

The Kraus operators for two photons can be constructed by taking tensor products of combinations of the set of single qubit Kraus operators as shown in Eq.(2). This parallel concatenation of multiple channels can be generalized for higher dimensional composite photon states [22]. Here we construct the Kraus operators for the two photon channel corresponding to Eq.(1).

$$K_i^2 \equiv \{K_i \otimes K_j : K_i, K_j \in \{K_i^1\}\}. \quad (2)$$

A set of projectors acting in the position Hilbert space are used to achieve the desired behaviour of noise.

$$\begin{aligned} P_{00} &= |0\rangle_1 |0\rangle_2 \langle 0|_1 \langle 0|_2 \\ P_{01} &= |0\rangle_1 |1\rangle_2 \langle 0|_1 \langle 1|_2 \\ P_{10} &= |1\rangle_1 |0\rangle_2 \langle 1|_1 \langle 0|_2 \\ P_{11} &= |1\rangle_1 |1\rangle_2 \langle 1|_1 \langle 1|_2. \end{aligned} \quad (3)$$

To construct the noise model, the single/two photon

noise Kraus operators are coupled with the appropriate projectors, and put together as a single set of combined Kraus operators \tilde{K}_i .

$$\tilde{K}_i \equiv \left\{ \begin{array}{ll} (K_i^1 \otimes I) \otimes P_{01}, & \text{(Single photon noise)} \\ (I \otimes K_i^1) \otimes P_{10}, & \\ (K_i^2) \otimes P_{00}, & \text{(Two photon noise)} \\ (I \otimes I) \otimes P_{11} & \text{(Identity channel)} \end{array} \right\}. \quad (4)$$

It can be verified that the action of the above Kraus operators satisfies all the required conditions of a quantum channel including the Complete Positivity and Trace Preserving (CPTP) condition. Note that this noise model does not accurately model the noise acting on the path states, since the projectors cause loss of correlations. But in this study we are only examining the polarization degree of freedom, hence this model is valid.

The noise model developed above is applied on the hyperentangled state of the form,

$$|\Psi\rangle_{HE} = \frac{1}{\sqrt{2}}(|H\rangle_1 |V\rangle_2 + |V\rangle_1 |H\rangle_2) \otimes (|1\rangle_1 |1\rangle_2 + |0\rangle_1 |0\rangle_2). \quad (5)$$

Here subscript 1 and 2 represent photon 1 and photon 2. In the above expression we can note that both the photon entangled in polarization degree of freedom take the same path in this configuration. However, the polarization degree entangled photons will remain spatially separated along each path. Such states can be generated in a laboratory setting by using the methods illustrated in references [20, 23]. Conventional polarization entangled photons that are coupled with only one of the spatial modes is used as a reference. For ease of comparing these states, the spatial mode of the conventional entangled photon pair is taken to be $|0\rangle_1 |1\rangle_2$. Now the path-polarization entangled and polarization entangled states belonging to $\mathcal{H}_{pol} \otimes \mathcal{H}_p$ can be written as,

$$|\Psi\rangle_{HE} = \frac{1}{\sqrt{2}}(|HV00\rangle + |HV11\rangle + |VH00\rangle + |VH11\rangle), \quad (6)$$

$$|\Psi\rangle_E = \frac{1}{\sqrt{2}}(|HV01\rangle + |VH01\rangle). \quad (7)$$

The Kraus operators act on the density matrices of the photon states. The corresponding density matrix representations of the photon states are,

$$\rho_{HE} = |\Psi_{HE}\rangle \langle \Psi_{HE}|, \quad \rho_E = |\Psi_E\rangle \langle \Psi_E|. \quad (8)$$

The action of the noise model is then given by,

$$\tilde{\rho}_{(HE)} = \sum_i \tilde{K}_i \rho_{(HE)} \tilde{K}_i^\dagger, \quad \tilde{\rho}_{(E)} = \sum_i \tilde{K}_i \rho_{(E)} \tilde{K}_i^\dagger. \quad (9)$$

Following this, the path degree of freedom is partial

traced out for both the states bringing down both of these states to a 4-dimensional space. This is done in order to compare among the entanglement in both these pairs of photons on an equal footing.

$$\rho_{\text{HE}}^{\text{out}} = \text{Tr}_{\text{POS}}(\tilde{\rho}_{(\text{HE})}), \quad \rho_{\text{E}}^{\text{out}} = \text{Tr}_{\text{POS}}(\tilde{\rho}_{(\text{E})}). \quad (10)$$

The controlled noise model can be used with any set of single qubit Kraus operators by substituting in place of Eq.(1) and getting the corresponding set of controlled Kraus operators \tilde{K} .

III. QUANTIFYING CORRELATIONS UNDER NOISE

There are many measures that can reliably quantify (quantum) correlations in a composite system [24–26]. To study the effect of noise on the quantum correlations of the photon states, we introduce an entanglement measure called negativity and a measure of nonlocality using the CHSH parameter. We will also take a look at entanglement witnesses which present an effective method to experimentally verify the presence of entanglement in the system.

A. Entanglement Negativity

Given a density matrix of a composite quantum system, the entanglement negativity \mathcal{N} between two bipartitions A:B of the system is given as,

$$\mathcal{N}(\rho) = \frac{\|\rho^{\Gamma_A}\|_1 - 1}{2}, \quad (11)$$

where $\|\rho^{\Gamma_A}\|$ denotes the partial transpose of ρ with respect to subsystem A, and $\|X\|_1 = \text{Tr}(\sqrt{XX^\dagger})$ denotes the trace-norm [26, 27]. For the path encoded state, the polarization degree of freedom of the two photons are considered as the subsystems. For the purpose of comparing conventional entangled photons and path-encoded photons, we trace out the position degree of freedom of the path-encoded state after applying the operations to it. Initially, it can be seen that the hyperentangled states have an entanglement negativity of $\mathcal{N} = 1$. The state of the hyperentangled photons in position degree of freedom contributes equally to the entanglement negativity as the polarization and can be added up using the additive property of negativity.

Entanglement Witness— Experimentally, it is difficult and resource intensive to measure entanglement negativity without knowing the complete density matrix of the state through methods like quantum state tomography (QST) [28]. For this reason we construct entanglement witness, which are operators whose expectation value can be used as an indicator for whether the state

is entangled or not [29]. These expectation values can be measured experimentally using fewer number of measurements as compared to QST. We study here theoretically how the expectation values of suitable witness operators are affected for various levels of noise, and illustrate a method to experimentally measure $\langle W \rangle$ using a few measurements [30]. A state ρ is entangled if and only if there exists a Hermitian operator W such that $\text{Tr}(\rho W) < 0$ and $\text{Tr}(\rho_{\text{sep}} W) \geq 0$ for all separable states ρ_{sep} . It should be noted that given an entanglement witness for a particular entangled state, it may not be a suitable witness for other entangled states.

B. Nonlocality Measurements

A useful benchmark for certification of entanglement in a system is the violation of the Bell's inequality [31]. (Clauser Horne Shimony Holt) CHSH inequality measurements can be performed in laboratory settings using an entangled photons pairs and local measurements using optical components like half-wave plates or polarizers, and coincidence detection's [32, 33]. We investigate the effect of the higher dimensional entanglement on the CHSH parameter S .

Given a bipartite quantum system, we can define two parties, Alice and Bob, who perform local measurements on one of the photons. They can choose from a set of orthogonal measurements independently. The CHSH inequality is given by,

$$S = E(a, b) - E(a, b') + E(a', b) + E(a', b'). \quad (12)$$

Here a/a' and b/b' represent the measurements with outcomes 1 or -1, taken by Alice and Bob respectively. $E(a, b)$ represent the expectation value for the measurement a and b . According to Bell's theorem of nonlocality, for physical systems that can be described by local hidden variable theories, the CHSH inequality is given by,

$$|S| \leq 2. \quad (13)$$

Quantum systems are known to violate the CHSH inequality, indicating the nonlocality of quantum mechanics. Here we theoretically investigate the Bell nonlocality of hyperentangled photons, under the effect of noise. As a reference, we also see the effect of noise on the nonlocality of conventional photons. In the context of photons, a/a' and b/b' are determined by the angles θ/θ' and δ/δ' for along which the polarization ($|H\rangle$ or $|V\rangle$) of the photon are measured.

In the experimental setting, measurements are made in the form of coincidence counts using suitable time tagging devices. The measurements are performed for 4 different orientations: $C_{HH}, C_{HV}, C_{VH}, C_{VV}$. Here C_{HV} stands for coincidence counts when first photon is measured for polarization H and the second photons measured for polarization V. Using these coincidence counts,

$E(\theta, \delta)$ can be obtained using,

$$E(\theta, \delta) = \frac{C_{HH} + C_{VV} - C_{HV} - C_{VH}}{C_{HH} + C_{VV} + C_{HV} + C_{VH}}. \quad (14)$$

S can now be computed using Eq.(12).

Theoretically the S parameter calculation can be done by obtaining the probability of measurements for various configurations, by either performing rotation operations on the density matrix or performing a measurement using a rotated projection operator. For the first case,

$$\begin{aligned} \rho_{rot}^{out} &= R(\theta) \otimes R(\delta) (\rho_{(E/HE)}^{out}) R(\theta) \otimes R(\delta), \\ P_{VV} &= \text{Tr}(\mathcal{P}_{VV} \rho_{rot}^{out}). \end{aligned} \quad (15)$$

Where R is the rotation operator acting on the polarization degree of freedom, and \mathcal{P}_{VV} denotes projection operator along the state $|VV\rangle$. Now,

$$E(\theta, \delta) = P_{HH} + P_{VV} - P_{HV} - P_{VH}. \quad (16)$$

The value of the CHSH parameter S, is calculated for different angles, keeping the angles θ and δ at a suitable fixed value and computing S for different values for θ' and δ' . In Fig. 1, the S parameter is plotted against θ' and δ' in the range $0 \leq \theta' \leq \pi$, $0 \leq \delta' \leq \pi$ and fixing $\theta = \pi/4$ and $\delta = \pi/3$. As a reference, S is plotted for zero noise level or an identity channel for polarization entangled photons.

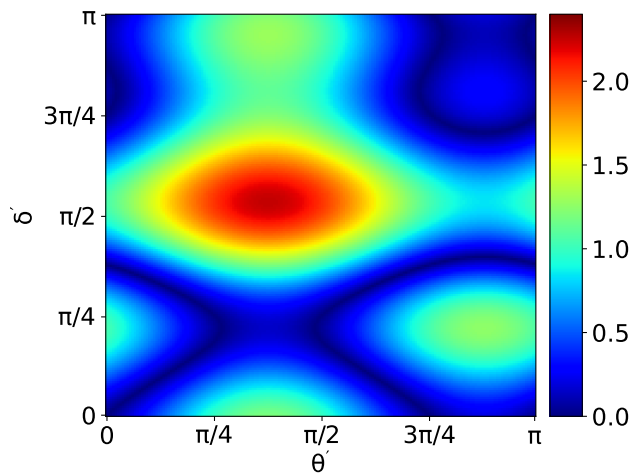


FIG. 1: Theoretical plot of nonlocality for the polarization entangled state. $\theta = \pi$ and $\delta = 7\pi/8$ is fixed and $S(\theta', \delta')$ is plotted. The deep red region indicates a maximum violation of CHSH inequality.

IV. RESULTS

In this section we study the affect of the noise model Eq.(4) on the the correlations of the photon states. Three different basic noise models are used here [21]: (1) bit flip

(2) depolarizing (3) phase damping. We numerically plot the variation of the quantifiers introduced in Sec. III as a function of the noise levels and compare the effect of noise on hyperentangled states and entangled states.

A. Bit Flip Noise

The bit flip noise channel as the name suggest is used to model bit flip errors in two level quantum systems. The noise parameter p in the context of bit flip noise is the probability of a flip ($|H\rangle \leftrightarrow |V\rangle$) occurring. The Kraus operators for the single qubit flip noise channel is given by,

$$K_1 = (p) \begin{pmatrix} 0 & 1 \\ 1 & 0 \end{pmatrix}, \quad K_2 = (1-p) \begin{pmatrix} 1 & 0 \\ 0 & 1 \end{pmatrix}. \quad (17)$$

On the action of the bit flip channel on the hyperentangled photons and the entangled reference states, the output state $\rho_{(E/HE)}^{out}$ is computed for various values of p. Here, p quantifies the amount of noise being acted on the photon states. $\mathcal{N}(\rho_{(HE)}^{out})$ and $\mathcal{N}(\rho_{(E)}^{out})$ can now be computed using Eq.(11).

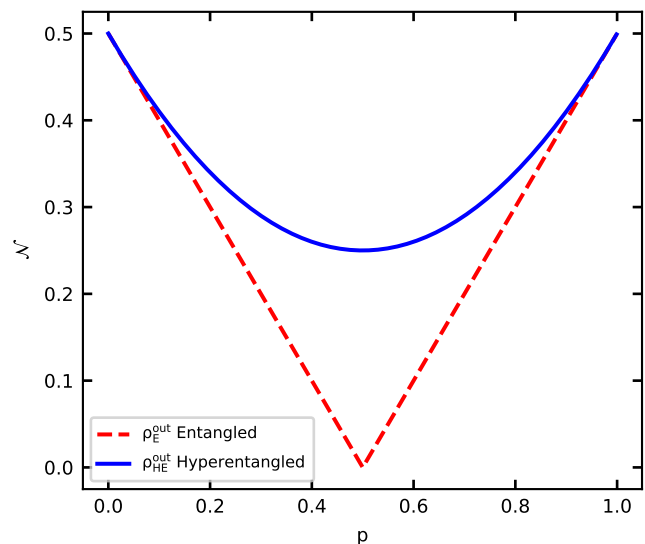


FIG. 2: Entanglement negativity \mathcal{N} plotted against the level of noise p for the bit flip noise channel. The plot for hyperentangled state shows a higher level of negativity than the plot for entangled state.

In Fig. 2, the plot for negativity shows enhanced retention of entanglement in hyperentangled states. The enhancement could possibly be the result of the state that was chosen that includes a superposition of the noisy and noiseless path, which reduces the effect of noise acting on the state. It can be observed that the value of negativity returns back to the highest value of $\mathcal{N} = 0.5$ possibly as the state now returns to the maximally entangled two

photon (Bell) state for $p = 1$.

Now for an entanglement witness as explained in the Sec. III, for the bit flip channel (with $0 \leq p \leq 0.5$) there exists a simple witness,

$$W = \frac{1}{2} \begin{pmatrix} 1 & 0 & 0 & 0 \\ 0 & 0 & -1 & 0 \\ 0 & -1 & 0 & 0 \\ 0 & 0 & 0 & 1 \end{pmatrix} \quad (18)$$

where W can be easily decomposed to a set of local measurements [30],

$$W = \frac{1}{2}(\sigma_i \otimes \sigma_i - \sigma_x \otimes \sigma_x - \sigma_y \otimes \sigma_y + \sigma_z \otimes \sigma_z). \quad (19)$$

Such a measurement can be performed in the laboratory using local measurements in the Pauli basis, and combining the results with the weights. The theoretical expectation value of W is plotted in Fig. 3. In the following subsections we see that the same entanglement witness Eq.(18) can be used as a witness.

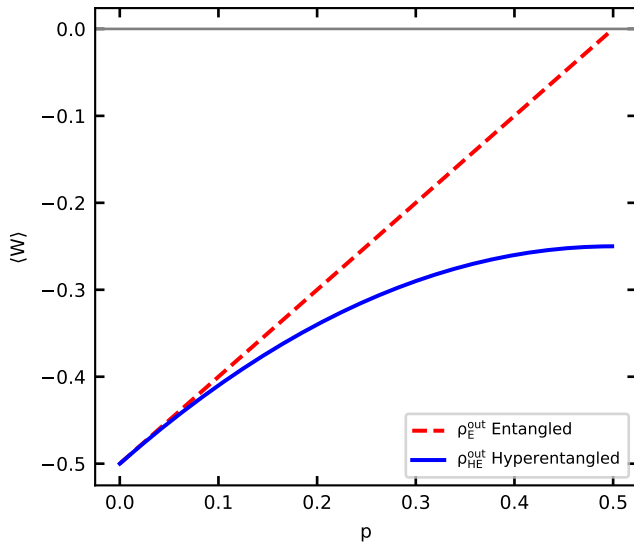


FIG. 3: $\langle W \rangle$ for noise levels $0 \leq p < 0.5$ of the bit flip channel. The expectation value of the witness for hyperentangled state has a negative value at $p = 0.5$ where the expectation value of witness for the entangled state becomes $\langle W \rangle = 0$ indicating the state becoming separable.

In the Fig. 3, it can be seen that both plots approach the value $\langle W \rangle$ with increasing levels of noise and at $p = 0.5$, the witness for the entangled state reaches $\langle W \rangle = 0$ indicating separability ($\mathcal{N} = 0$), but the hyperentangled state has negative value of $\langle W \rangle$ indicating entanglement, which is in agreement with the negativity plot Fig. 2. Although, $\langle W \rangle$ does not explicitly quantify entanglement, it can be used to comparatively illustrate the robustness of the states against noise.

For the nonlocality measurements we compute the theoretical value of quantity S as explained in Sec. III B. The

$S(\theta', \delta')$ value for $\theta = \pi$ and $\delta = 7\pi/8$ is computed for ρ_E^{out} and ρ_{HE}^{out} for the bit flip channel with a fixed value of $p = 0.5$. There is a visible difference in the pattern between ρ_E^{out} and ρ_{HE}^{out} in the Fig. 4, but it does not give much insight into the difference between the two channels. However, there is no violation of CHSH inequality in this range indicating that the noise has degraded the nonlocality of both the states.

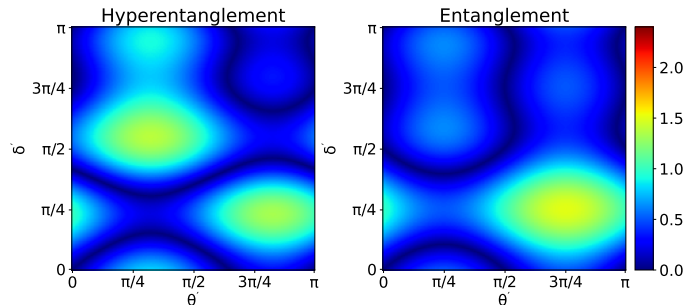


FIG. 4: Non locality plots for the bit flip channel with $p = 0.5$. $\theta = \pi$ and $\delta = 7\pi/8$ is fixed and θ' and δ' are varied. A difference in the pattern of the maximum nonlocality is seen. It is evident that the bit flip noise has degraded the nonlocality in both states when compared with Fig. 1.

Although it is clear from the plots that the presence of noise affects the nonlocality of the states, the nature of this effect cannot be conclusively obtained. For a better comparison of the nonlocality of ρ_{HE} and ρ_E the maximum value of S in the range $0 \leq \theta, \delta \leq \pi$ with $\theta' = \pi/2$ and $\delta' = \pi/4$ is plotted. The plots in Fig. 5 show the variation in the maximum violation in S in the given range of θ and δ with the noise parameter p for the discussed noise models for the given angles. Contrary to negativity plots, there seems to be not much of a higher nonlocality in either of the cases, possibly because bit flip noise affects nonlocality for both the states in a similar manner. In an experimental setting it may be difficult to iterate over all the possible angles to compute the S value and find the maximum value, but the plots in Fig. 1 and other such plots will be a good reference to identify the regions where maximum S can be obtained.

B. Depolarizing Noise

This noise channel is similar to the Bit flip channel. It is a combination of bit flip, phase flip, and bit + phase flip (represented by Pauli matrices). The noise parameter here serves as probability of the flips. The single qubit Kraus operators for the depolarizing noise channel are,

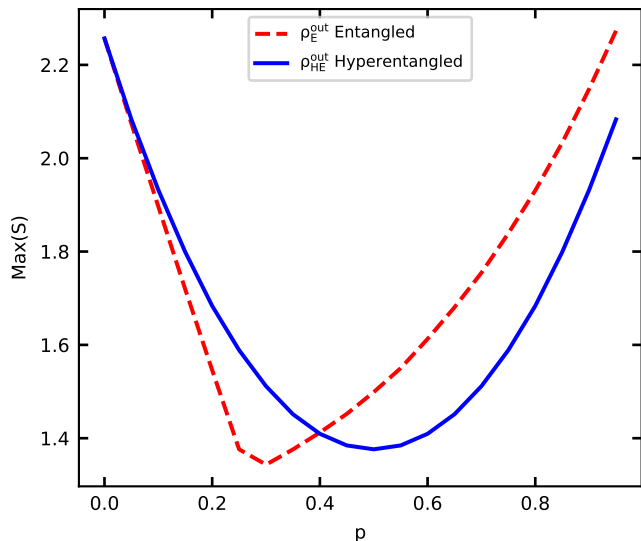


FIG. 5: $\text{Max}(S)$ vs. Bit flip noise level p for $\theta = \pi/2$ and $\delta = \pi/4$ and $\theta', \delta' \in [0, \pi]$. The maximum value of S , is seen to follow a similar trend in both the cases.

$$\begin{aligned}
 K_1 &= (p/3) \begin{pmatrix} 0 & 1 \\ 1 & 0 \end{pmatrix} & K_2 &= (p/3) \begin{pmatrix} 1 & 0 \\ 0 & -1 \end{pmatrix} \\
 K_3 &= (p/3) \begin{pmatrix} 0 & i \\ -i & 0 \end{pmatrix} & K_4 &= (1 - 3p/4) \begin{pmatrix} 1 & 0 \\ 0 & 1 \end{pmatrix}
 \end{aligned} \tag{20}$$

The corresponding negativity and witness plots Fig. 6, Fig. 7 shows the clear advantage of hyperentangled states. Entanglement is degraded relatively less in hyperentanglement for the case of depolarizing noise. The witness operator used here is the same as the witness of bit flip channel Eq.(18). As the witness is the same we are able to use the same decomposition in Eq.(19) for it. In Fig. 7, $\langle W \rangle$ for the ρ_E^{out} can be seen to approach $\langle W \rangle = 0$ with increasing noise levels and eventually crosses it at the same level of noise for which $\mathcal{N} = 0$, indicating that the state is now separable. But for ρ_{HE}^{out} , $\langle W \rangle < 0$ throughout the noise levels. This agrees with the corresponding entanglement negativity plot of the depolarizing channel.

The nonlocality plots Fig. 8, Fig. 9 also show a clear advantage for hyperentanglement, indicating enhanced retention of nonlocality through depolarizing channel.

C. Phase Damping Noise

The phase damping noise channel is used to model the loss of a fixed relative phase between the states of a quantum system, due to interactions with the environment. This process also termed as decoherence, is a frequently

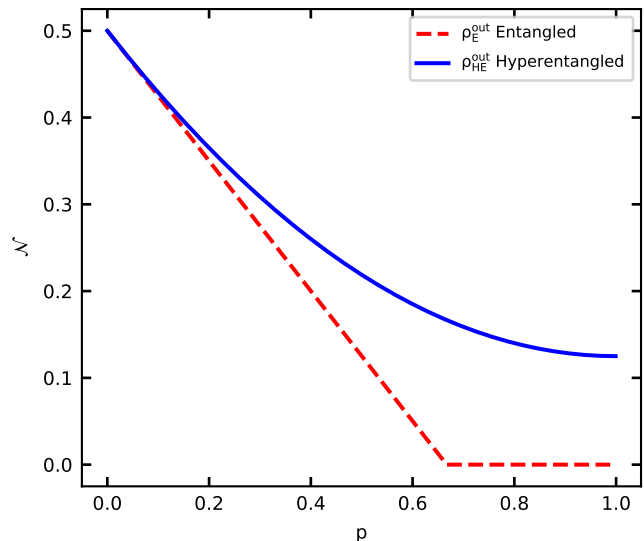


FIG. 6: Entanglement negativity \mathcal{N} plotted against the level of noise p for the depolarizing noise channel. The negativity of the entangled state reaches zero faster than the hyperentangled state, indicating an enhancement.

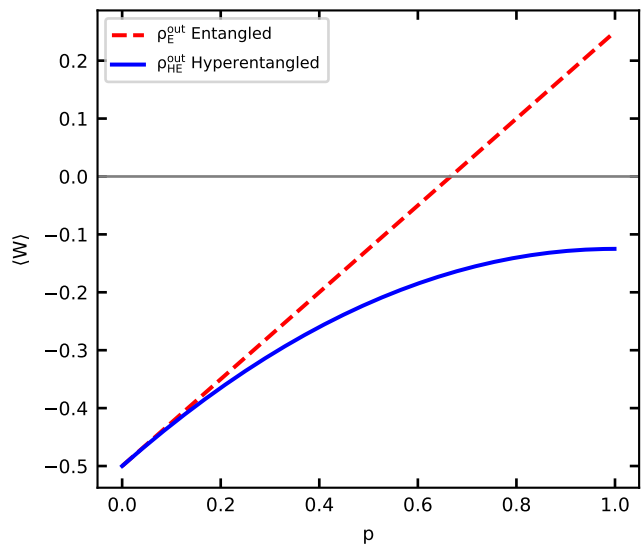


FIG. 7: $\langle W \rangle$ for different levels of noise for the depolarizing channel. The plot for the entangled state reaches $\langle W \rangle = 0$ at the same level of p for which $\mathcal{N} = 0$, and the plot for hyperentangled state remains in the negative region for all levels of noise.

encountered effect in photons. The Kraus operators for the phase damping noise model are,

$$K_1 = \begin{pmatrix} 1 & 0 \\ 0 & \sqrt{1-p} \end{pmatrix} \quad K_2 = \begin{pmatrix} 0 & 0 \\ 0 & \sqrt{p} \end{pmatrix}. \tag{21}$$

Similar to the previous models, plots for the quanti-

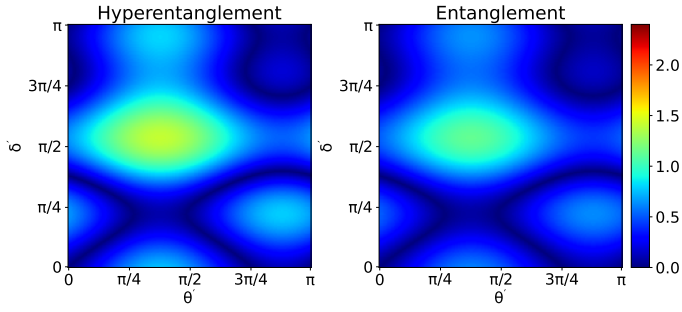


FIG. 8: Non locality plots for the depolarizing noise channel with $p = 0.5$. $\theta = \pi$ and $\delta = 7\pi/8$ is fixed and θ' and δ' are varied, Both the plots have a similar pattern with a slightly decreased S value for the entangled state.

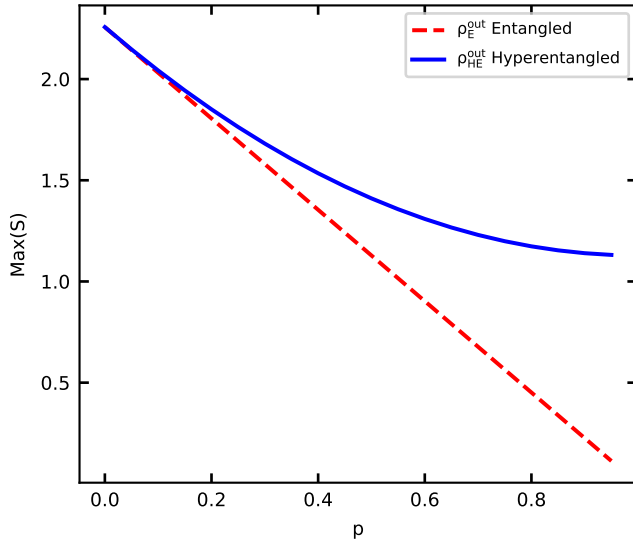


FIG. 9: Max(S) vs. Depolarizing noise level p for $\theta = \pi/2$ and $\delta = \pi/4$ and $\theta', \delta' \in [0, \pi]$. The plot for hyperentangled state shows a higher level of nonlocality compared to the entangled state.

fiers are plotted for the phase damping noise channel. In the negativity and witness plots Fig. 10, Fig. 11. Hyperentangled states shows a slight advantage as compared to the entangled state.

However, for the phase damping noise channels, it can be seen that both the states undergoing phase damping noise still violates the CHSH inequality. The plots obtained in Fig. 12 indicates that the phase damping channel has a negligible effect on the nonlocality of a quantum state.

As seen in the nonlocality plots for the phase damping noise channel, the S parameter remains above 2 for all the noise levels except $p = 1$, which is complete decoherence. The decohered state, is now a classical state which saturates the CHSH inequality $S = 2$.

In the case of the phase damping noise there appears to be only a minor difference between the nonlocality of $\rho_{(E)}^{out}$

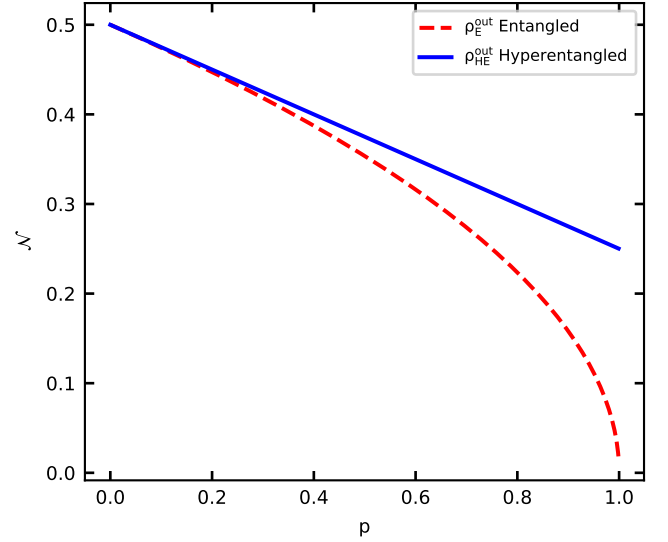


FIG. 10: Entanglement negativity \mathcal{N} plotted against the level of noise p for the phase damping noise channel. The negativity for hyperentangled state is slightly higher compared to the entangled state with the difference increasing for higher levels of noise.

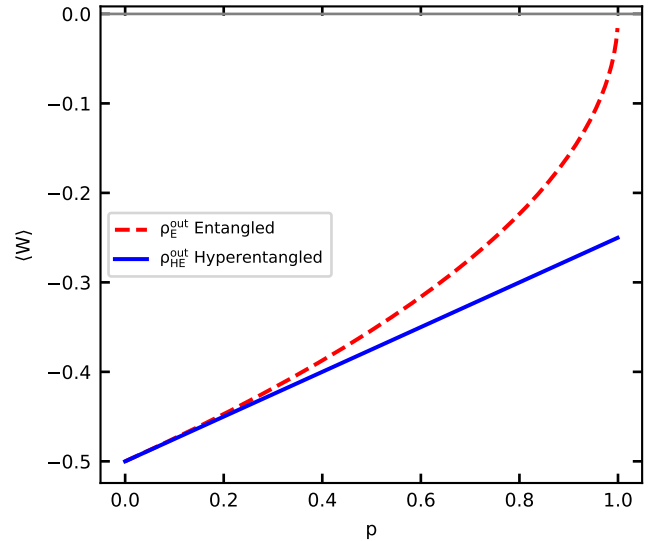


FIG. 11: $\langle W \rangle$ for different levels of noise of the phase damping channel, The plots are consistent with the negativity plot Fig. 10 showing a similar inverse trend.

and $\rho_{(HE)}^{out}$. This difference may possibly be negligible to be detected in a laboratory setting.

D. Unitary Noise Model

The Kraus operators of a noise channel can be used to back calculate an equivalent unitary that acts on a sys-

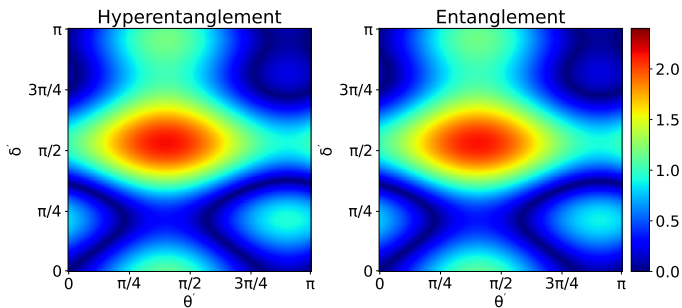


FIG. 12: Non locality plots for the phase damping channel with $p = 0.5$. $\theta = \pi$ and $\delta = 7\pi/8$ is fixed and θ' and δ' are varied. Both plots show a negligible difference compared to each other and the zero noise case Fig. 1.

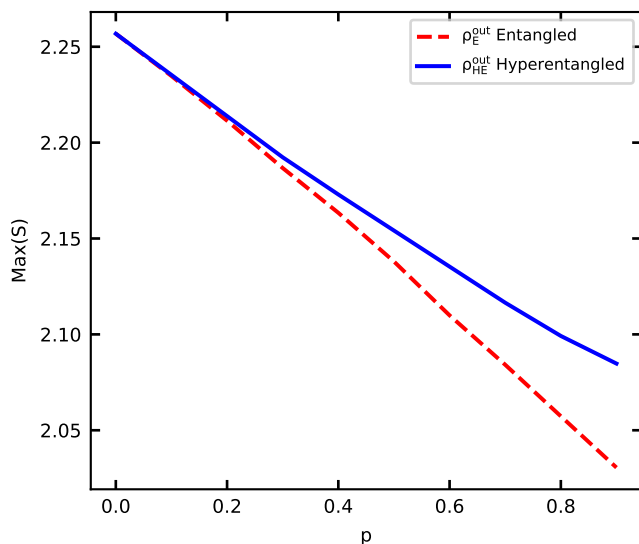


FIG. 13: Max(S) vs. Phase damping noise level p for $\theta = \pi/2$ and $\delta = \pi/4$ and $\theta', \delta' \in [0, \pi]$. Both the plots show a downtrend, but the maximum S value still violate CHSH inequality for both the plots.

tem coupled with the environment. This unitary gives an equivalent dynamics to the noise channel when environment is traced out. This method termed as stinespring dilation is given by,

$$U_{A \rightarrow A'E} : |\psi\rangle \rightarrow \sum_a K_a |\psi\rangle \otimes |a\rangle, \quad (22)$$

where E corresponds to the environment coupled with the system A with dimension equal to the number of Kraus operators and orthonormal basis $\{|a\rangle\}$.

We construct a dilated unitary for the bit flip channel,

$$U_x = \begin{pmatrix} \sqrt{1-p} & 0 & 0 & \sqrt{p} \\ 0 & \sqrt{1-p} & \sqrt{p} & 0 \\ 0 & -\sqrt{p} & \sqrt{1-p} & 0 \\ -\sqrt{p} & 0 & 0 & \sqrt{1-p} \end{pmatrix}. \quad (23)$$

Now using a controlled Unitary as given by,

$$U = P_{00} \otimes (U_x \otimes U_x) + P_{01} \otimes (U_x \otimes I) + P_{10} \otimes (I \otimes U_x) + P_{11} \otimes (I \otimes I). \quad (24)$$

The advantage of using this method is that we can also see the variation of correlations in path (entanglement) with the noise. After applying the Unitary U to the system environment state the environment is traced out, and negativity is calculated of the polarization and path degree of freedom of the resultant state. The correlations in path is calculated by partial tracing out polarization degree of freedom of the resultant state.

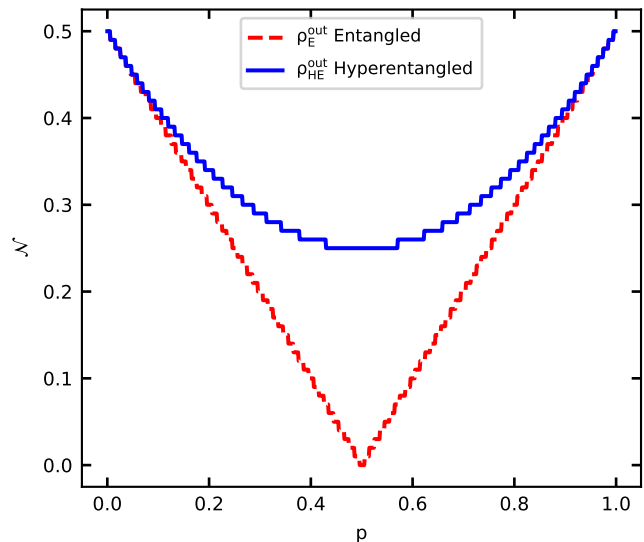


FIG. 14: Negativity in the polarization degree of freedom vs noise level p for the bit flip channel using stinespring dilation. The plot is equivalent to the negativity plot obtained for the bit flip channel Fig. 2

The plot of negativity of polarization degree of freedom in Fig. 14 is identical to the plot for negativity in Fig. 2. We also observe an inverse linear relation of the negativity of the path state and the noise level p .

V. CONCLUSION

The noise model proposed in this paper serves as a useful tool to theoretically study the effect of various types of noises encountered in the experimental settings where one of the basis state of an entangled pair is subject to noise. One of the main features of a quantum systems that sets it apart from a classical systems are the quantum correlations, and these correlations have been proven to be a useful resources in many applications which utilise quantum systems. Higher dimensional entanglement, have proven their advantages over conventional entanglement in many such applications. The results obtained here path-polarization hyper entangled

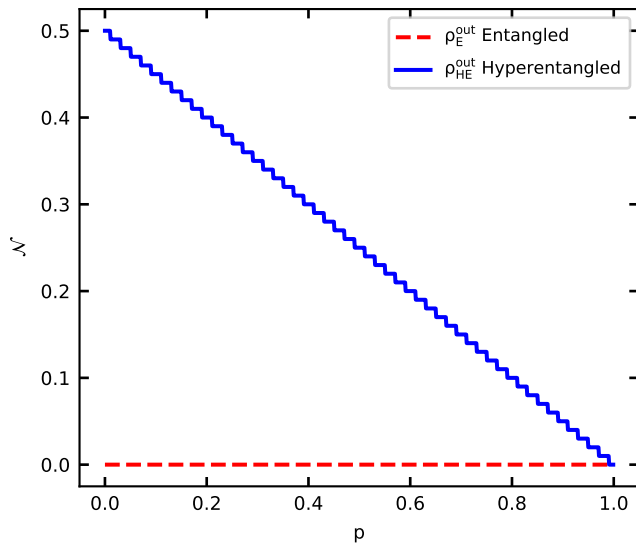


FIG. 15: Negativity in the path DOF vs noise level p for the bit flip channel using stinespring dilation. The negativity in the entangled state remains at 0 owing to no path entanglement, and the negativity for hyperentangled state shows an inverse linear trend with the noise level

state help confirm this advantage and possibly provides a reason for it. The entanglement in the path, provides a way to retain better correlations through a noisy environment of the form discussed here. The hyperentangled states are shown to have enhanced negativity as compared to the conventional entangled state. An experimental method to confirm this is provided in the form of entanglement witnesses, that provide a method to verify whether a state is entangled or not using few joint local measurements. The CHSH parameter violation is also computed and it shows that hyperentangled states retain nonlocality as good as, or better than entangled states. It can be concluded that path-polarization hyperentangled state Eq. (5) can be used as robust probe in a noisy environment for applications like quantum communication and quantum illumination.

Acknowledgement. We acknowledge the support from the Office of Principal Scientific Advisor to Government of India, project no. Prn.SA/QSim/2020.

-
- [1] R. Horodecki, P. Horodecki, M. Horodecki, and K. Horodecki, Quantum entanglement, *Rev. Mod. Phys.* **81**, 865 (2009)
- [2] V. Giovannetti, S. Lloyd, and L. Maccone, Advances in quantum metrology, *Nat. Photonics* **5**, 222–229 (2011)
- [3] A. Ekert, Quantum cryptography based on Bell’s theorem, *Phys. Rev. Lett.* **67**, 661 (1991).
- [4] C. H. Bennett and S. J. Wiesner, Communication via one- and two-particle operators on Einstein-Podolsky-Rosen states, *Phys. Rev. Lett.* **69**, 2881 (1992)
- [5] S. Lloyd, Enhanced Sensitivity of Photodetection via Quantum Illumination, *Science* **321** 5895, (2008).
- [6] C. H. Bennett, G. Brassard, C. Crépeau, R. Jozsa, A. Peres, and W. K. Wootters, Teleporting an unknown quantum state via dual classical and Einstein-Podolsky-Rosen channels, *Phys. Rev. Lett.* **70**, 1895 (1993)
- [7] R. Jozsa and N. Linden, On the role of entanglement in quantum-computational speed-up, *Proc. Math. Phys. Eng. Sci.* **459**, 2036 (2003)
- [8] A. Acín, N. Brunner, N. Gisin, S. Massar, S. Pironio, and V. Scarani, Device-Independent Security of Quantum Cryptography against Collective Attacks, *Phys. Rev. Lett.* **98**, 230501
- [9] A.V. Prabh, B. Suri, and C.M Chandrashekar, Hyperentanglement-enhanced quantum illumination, *Phys. Rev. A* **103**, 052608 (2021)
- [10] J.T. Barreiro, T.C. Wei, and P.G. Kwiat, Beating the channel capacity limit for linear photonic superdense coding, *Nature Physics* **4**, pages 282–286 (2008)
- [11] N. J. Cerf, M. Bourennane, A. Karlsson, and N. Gisin, Security of Quantum Key Distribution Using d-Level Systems, *Phys. Rev. Lett.* **88**, 127902 (2002)
- [12] F. Zhu, M. Tyler, N. H. Valencia, M. Malik, and J. Leach, Is high-dimensional photonic entanglement robust to noise? *AVS Quantum Sci.* **3**, 011401 (2021)
- [13] D. Collins, N. Gisin, N. Linden, S. Massar, and S. Popescu, Bell Inequalities for Arbitrarily High-Dimensional Systems, *Phys. Rev. Lett.* **88**, 040404 (2002)
- [14] P.G Kwiat., K. Mattle, H. Weinfurter, A. Zeilinger, A.V. Sergienko, and Y. Shih, New High-Intensity Source of Polarization-Entangled Photon Pairs, *Phys. Rev. Lett.* **75**, 4337 (1995)
- [15] P. G. Kwiat, Hyper-entangled states, *J. Mod. Opt.* **44** 2173 (1997)
- [16] J. T. Barreiro, N. K. Langford, N. A. Peters, and P. G. Kwiat, Generation of Hyperentangled Photon Pairs, *Phys. Rev. Lett.* **95**, 260501 (2005)
- [17] T.-M. Zhao, Y. S. Ihn, and Y.-H. Kim, Direct Generation of Narrow-band Hyperentangled Photons, *Phys. Rev. Lett.* **122**, 123607
- [18] S. Dong et al., Generation of hyper-entanglement in polarization/energy-time and discrete-frequency/energy-time in optical fibers, *Sci. Rep.* **5**, 9195 (2015)
- [19] P. A. A. Yasir and C. M. Chandrashekar, Generation of hyperentangled states and two-dimensional quantum walks using J or q plates and polarization beam splitters, *Phys. Rev. A* **105**, 012417 (2022)
- [20] M. Barbieri, C. Cinelli, P. Mataloni, and F. De Martini, Polarization-momentum hyperentangled states: Realization and characterization, *Phys. Rev. A* **72**, 052110 (2005)
- [21] M. A. Nielsen and I. L. Chuang, Quantum computation and quantum information. Cambridge Cambridge University Press, 2019.
- [22] M. Wilde, Quantum information theory. Cambridge University Press, 2013.

- [23] C. Simon and J.-W. Pan, Polarization Entanglement Purification using Spatial Entanglement, *Phys. Rev. Lett.* **89**, 257901
- [24] H. Ollivier and W. H. Zurek, Quantum Discord: A Measure of the Quantumness of Correlations, *Phys. Rev. Lett.* **88**, 017901
- [25] S. Hill and W. K. Wootters, Entanglement of a Pair of Quantum Bits, *Phys. Rev. Lett.* **78**, 5022 (1997)
- [26] G. Vidal and R. F. Werner, Computable measure of entanglement, *Phys. Rev. A* **65**, 032314 (2002)
- [27] K. Życzkowski, P. Horodecki, A. Sanpera, and M. Lewenstein, Volume of the set of separable states, *Phys. Rev. A* **58**, 883 (1999)
- [28] D. F. V. James, P. G. Kwiat, W. J. Munro, and A. G. White, Measurement of qubits, *Phys. Rev. A* **64**, 052312 (2001)
- [29] B. M. Terhal, Bell inequalities and the separability criterion, *Physical Letters A* **271** 5-6 (2000)
- [30] O. Gühne, P. Hyllus, D. Bruss, A. Ekert, M. Lewenstein, C. Macchiavello, A. Sanpera, Detection of entanglement with few local measurements, *Phys. Rev. A* **66**, 062305
- [31] J. S. Bell, On the Einstein Podolsky Rosen paradox, *Physics Physique Fizika* **1**, 195
- [32] A. Aspect, P. Grangier, and G. Roger, Experimental Tests of Realistic Local Theories via Bell's Theorem, *Phys. Rev. Lett.* **47**, 460 (1981)
- [33] J. F. Clauser, M. A. Horne, A. Shimony, and R. A. Holt, Proposed Experiment to Test Local Hidden Variable Theories., *Phys. Rev. Lett.* **23**, 880 (1970)